Energy Conversion and Management 88 (2014) 259–266

Contents lists available at ScienceDirect

Energy Conversion and Management

journal homepage: www.elsevier.com/locate/enconman

Pyrolysis kinetics of spent lark mushroom substrate and characterization of bio-oil obtained from the substrate

Haifeng Jiang [a], Zhiqiang Cheng [b], Tianqi Zhao [a], Mengzhu Liu [a], Mingyue Zhang [a], Jianing Li [a], Meijuan Hu [a], Li Zhang [a], Junfeng Li [a,*]

[a] College of Chemistry, Jilin University, Changchun 130012, PR China
[b] College of Resources and Environment, Jilin Agriculture University, Changchun 130118, PR China

ARTICLE INFO

Article history:
Received 16 April 2014
Accepted 7 August 2014

Keywords:
Pyrolysis
Kinetics
Bio-oil
Spent lark mushroom substrate
Renewable energy

ABSTRACT

In our work, thermal behavior and kinetic characteristics of spent lark mushroom substrate were evaluated to elaborate the thermal decomposition mechanisms and explore the influence of heating rate by using thermogravimetric analyzer and Coats–Redfern method. The study of pyrolysis temperature of raw material was also operated at the range of 410–530 °C, under the feeding rate 0.36 g/min, and the nitrogen flow 16 L/h. The results showed that the maximum bio-oil yield was obtained at 470 °C with the yield of 14.4 wt.%. The analysis of Fourier transform infrared spectrometer and gas chromatography coupled with mass selective detector indicated that the target liquid production was consisted of phenols, hydrocarbons and other components. Simultaneously, the low oxygen and high hydrogen content in bio-oil was also determined by elemental analysis. Based on the above-mentioned results, we demonstrated that the bio-oil obtained from the substrate had high utilization value as a potential energy resource.

1. Introduction

With the continuous consumption of fossil fuels, energy crisis and environmental issues have become more and more prominent. Hence, the utilization of renewable resources is of growing importance. Among the various forms of energy supply materials, biomass is always considered to be an important potential source [1]. In China, the growth rate of spent mushroom substrate is more than 8 million tons per annum and it may increase continuously in the future [2]. Unfortunately, a large number of residues tend to be incinerated or dumped as organic wasters to decompose naturally [3]. Particularly, spent lark mushroom substrate (SLMS) is often burned in the field, which brings negative impact on the environment due to the release of smoke and dust.

To date, pyrolysis, as one of the most important thermochemical methods, has been applied in the conversion of biomass and biomass wastes. According to the pyrolytic process, these solid residues can be converted into different phases, such as bio-oil, char, and gas [4,5]. In comparison with solid fuels, the liquids have many advantages, such as high energy density, easy storage and transport. The high calorie value and low ash content in bio-oil, which provide the potential to be mixed with conventional petroleum fuels [6]. Besides, bio-oil is also a kind of feedstock to produce high-value added chemicals. The byproduct, bio-char, can act as the soil modifier to improve the habitat of plants and enhance carbon sequestration [7,8]. Gas is also utilized by taking advantages of abundant gas types [9].

In order to obtain high energy conversion efficiency, the pyrolysis experiments of various biomasses have been carried out under different conditions. A clear brief containing the different experiment conditions and the main characteristics of bio-oil obtained from agriculture and forestry residues, is given in Table 1. These researches are of great helpful to promote the development of biomass thermochemical system. Additionally, pyrolysis kinetics also plays an important role in understanding the mechanism of solid-state thermal decomposition. Sait et al. [10] investigated the pyrolysis kinetics of date palm biomass. Their work showed that the highest conversion efficiency of raw material occurred at the temperature range of 200–450 °C, and the heat and mass transfer limitations may influence the thermal degradation of biomass in the absence of oxygen. Huang et al. [11] had concerned the pyrolysis behaviors of coffee hulls, bamboo leaves, sugarcane bagasse, and sugarcane peel. According to semi-quantitative method, a good linear regression was obtained in their work. Besides, the thermal

* Corresponding author. Tel.: +86 0431 85164704.
E-mail addresses: jianghaifeng11@126.com (H. Jiang), czq5974@163.com (Z. Cheng), zhaotq@jlu.edu.cn (T. Zhao), liumengzhu125@163.com (M. Liu), zhangmingyue8803@163.com (M. Zhang), 591115394@qq.com (J. Li), 442675083@qq.com (M. Hu), 805944538@qq.com (L. Zhang), jfli@jlu.edu.cn (J. Li).

http://dx.doi.org/10.1016/j.enconman.2014.08.006
0196-8904/

Table 1
Characteristics of bio-oils obtained from various biomasses under different experiment conditions.

Biomass	Experiment condition	Characteristic	Refs.
Sawdust	Pyrolysis occurred in the fixed-bed system	The obtained bio-oil had low pH value	[13]
Oreganum stalk	Pyrolysis was performed at 500 °C in a fluidized bed reactor	The bio-oil had high oxygen content	[14]
Rice straw	Pyrolysis was carried out at different temperatures	The maximum yield was determined at 450–750 °C	[15]
Palm oil decanter cake	Vacuum pyrolysis	The bio-oil had no tendency to polymerize at high temperature zone(above 500 °C)	[16]
Corn stalk	Pyrolysis in the presence of catalyst	The use of catalyst had increased the content of aromatic compounds in the oil	[17]

decomposition process of hazelnut husk was described in the study of Ceylan et al. From their paper, kinetics analysis results showed a good agreement with experimental data, which provided some references for future application [12].

Although spent lark mushroom substrate has abundant recycling utilization values, few researches are focused on its pyrolysis behavior and characterization of the obtained liquid production. In this paper, the pyrolysis behavior of the SLMS is investigated sufficiently. The related kinetic parameters are calculated by an iso-conversional model. Moreover, the characterization of liquid production is tested by different analysis means. Our work mainly aims to exposit pyrolytic characteristics of raw material, as well as provide some references for future application of liquid production.

2. Materials and methods

2.1. Preparation of raw material

The raw material was obtained from Changchun in Jilin province, China. After washing away the dirt on the surface of raw material, the dried solids were crushed by grinding machine. And then, a standardized sieve was used to obtain specifies desired particle size (<1 mm). The final samples were kept in a wide mouthed bottle at room condition.

2.2. Pyrolysis process of SLMS

Thermal analysis: the pyrolysis process was performed by the HTG-2 model Henven thermogravimetric analyzer. The samples (8–10 mg) distributed uniformly in crucible were heated from room temperature to 800 °C at different heating rates (5, 10, 15, 20 °C/min). As carrier gas, the constant flow rate of nitrogen atmosphere was fixed at 50 ml/min. The purposes of these measures were to eliminate the effect of eventual side reactions, and make mass and heat transfer limitation to the minimum. In addition, the initial and the final weight were recorded in each experiment to calculate the kinetic parameters.

Pyrolysis experiment: the experiments were carried out in a self-made pyrolyzer, which had been shown in Fig. 1. The pyrolyzer was mainly comprised of feeding section, pyrolysis zone and receiver. A screw feeder was installed at one side of feeding section. With the rotation of the adjustable speed motor and gear reducer, about 50 g SLMS particles for each experiment were constantly driven into the pyrolysis zone. The pyrolysis zone was made up of two heating jackets, which totally had length of 170 mm and inner diameter of 20 mm. In order to control the temperature accurately, thermocouples were put into the inner side of the heating jackets. At the end of pyrolysis zone, a vertical orientation counter-current condenser tube was connected, so that the temperature of condenser was maintained at around 282.15 K. The receiver was submerged in the icy debris container, which could ensure the condensation of bio-oil vapor sufficiently. Meanwhile, the non-condensable gases were collected in a Teflon bag and disposed in the future. The flow rate of nitrogen was kept at 16 L/h. Preliminary tests at different gas flow rates had demonstrated that the chosen gas flow rate could avoid gas condensation in solid collector and assure hypoxia environment in the whole process of the experiment.

For making the aqueous and oil phase separate, methylbenzene as the extraction agent was added into the liquid productions. Through the distillation process, an azeotrope composed of aqueous phase and methylbenzene, was distilled out in a calibrated glass tube. After standing for some time, the content of aqueous phase was measured with volumetric method. The mass of bio-oil was determined by calculating the weight change before and after distillation. The residual solids were collected in a solid collector and weighted as char. The final yields of the obtained bio-oil and char were calculated by Eq. (1).

$$Y = \frac{M_1}{M_2} \times 100\% \tag{1}$$

where Y was the yield, M_1 was the mass of the desired product, and M_2 was the initial mass of SLMS. The yield of gas was calculated by difference. The same experiment was operated at least twice in order to ensure availability of the data.

2.3. Kinetics study

Kinetics was widely applied in the design of thermochemical system, and some models to calculate the kinetic parameters had already been reported. An iso-conversional model, Coats–Redfern method [12], was used in the present work to obtain the parameters of main thermal stages of raw material and investigate the effect of heating rate. Moreover, the thermal disintegration process of biomass was considered to be a parallel first-order reaction, which was always used by other researchers [18–20].

The pyrolysis reaction equation could be described by the expression:

$$\frac{dx}{1-x} = \frac{A}{\phi} \exp\left(-\frac{E}{RT}\right) dT \tag{2}$$

where A was the pre-exponential factor, E was the apparent activation energy, ϕ was a linear heating rate for non-isothermal conditions, R was the gas constant and T was the absolute temperature. Moreover, x was the extent of raw material weight loss, which was calculated by Eq. (3):

$$x = \frac{W_o - W_t}{W_o - W_f} \tag{3}$$

where W_o was the initial mass, W_t was the mass at time t and W_f was the final mass at the end of pyrolysis process.

Upon integration the left and right sides of Eq. (2), the formula was written as follows:

$$\int_0^x \frac{dx}{1-x} = \frac{A}{\phi} \int_{T_o}^{T} \exp\left(-\frac{E}{RT}\right) dT \tag{4}$$

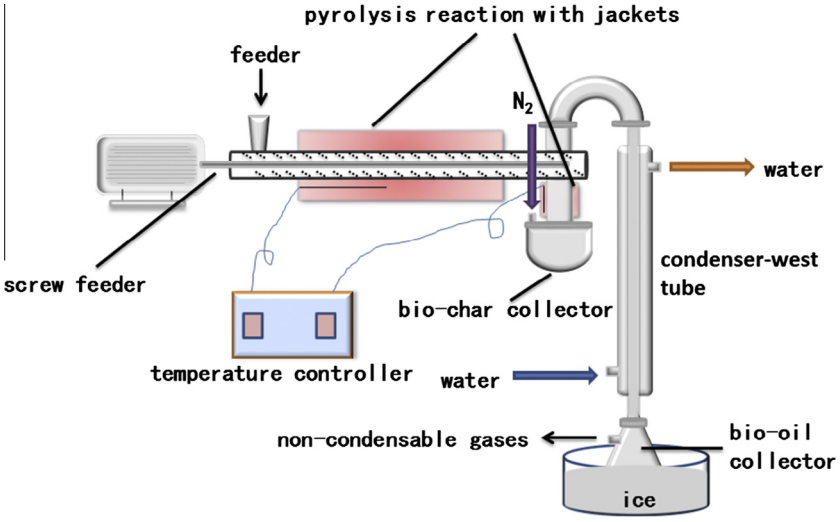

Fig. 1. Schematic diagram of the pyrolyzer.

Here, an assumption was given that x was zero, when the reaction was not start. The reaction equation could become the following expression:

$$\ln(1-x) = T^2\left(\frac{AR}{\phi E}\bullet\frac{E-2RT}{E}\right)\exp\left(-\frac{E}{RT}\right) \quad (5)$$

Logarithmic form on both sides, the final expression was described by Eq. (6):

$$\ln\left[-\frac{\ln(1-x)}{T^2}\right] = -\frac{E}{RT} + \ln\frac{AR}{\phi E} \quad (6)$$

A straight line was obtained by plotting the left side of Eq. (6) versus $\frac{1}{T}$, and Eq. (6) could be regarded as a linear equation. Here, the values of x and T were determined by TG data. Based on these, the activation energy E and pre-exponential factor A could be obtained easily.

2.4. Analysis methods

The volatiles and fix carbon content in the SLMS were determined by the TG data. The ash was obtained from the mass percentage of the solid residues after the combustion of raw material at 600 °C for 8 h. The carbon (C), hydrogen (H) and nitrogen (N) content in the raw material and the obtained bio-oil were determined by Vario EL Cube Elementar. Since it had been reported that the most parts of the biomass contained low sulfur content [12,13,21], we ignored the sulfur (S) content in samples. The oxygen (O) content was calculated by taking the difference. The higher heating value (HHV) and lower heating value (LHV) was respectively calculated by the following expressions [22,23].

$$\mathrm{HHV(MJ/kg)} = -1.3675 + 0.3137\mathrm{C} + 0.7009\mathrm{H} + 0.0318\mathrm{O} \quad (7)$$

$$\mathrm{LHV(MJ/kg)} = \mathrm{HHV} - 2.442 \times 8.936(\mathrm{H}/100) \quad (8)$$

In order to investigate the functional groups in feedstock and pyrolysis production, the Fourier transform infrared spectra (FT-IR) was recorded at the scan range from 400 to 4000 cm^{-1} by using the SHIMDZU 1.50SU1 FT-IR spectrometer. The spectral resolution was 4 cm^{-1}. Gas chromatography coupled with mass selective detector (GC/MS) was performed on Agilent 7890 gas chromatograph equipped with the Agilent 5975 N mass spectrometer. The National Institute of Standards and Technology mass spectrum library search (Version 2.0) was used to analyze the obtained spectra.

3. Results and discussion

3.1. Characteristics of raw material

The results of proximate and ultimate analyses of SLMS were listed in Table 2. From the table, the low moisture content (about 10%) in the feedstock indicated the time of the drying process could be shortened, which was favorable to conserve energy in the industrialized production process of bio-oil. Meanwhile, the higher heating value and the lower heating value were calculated by Eqs. (7) and (8), with the results of 16.62 and 15.55 MJ/kg, respectively. These data approximated those reported in agriculture residues, such as sweet sorghum bagasse (18.57, 17.30 Mg/kg) [1] and rice husk (16.8, 15.6 Mg/kg) [24]. It demonstrated that the SLMS, as well as other biomass, could be considered as the candidate for thermal energy production.

3.2. Pyrolysis behavior of SLMS

The thermogravimetric (TG) and differential thermogravimetric (DTG) curves of SLMS under the nitrogen atmosphere at different heating rates were shown in Fig. 2. From the figure, a dehydration process was observed clearly. With the increasing of heating rate, the dehydration stage occurred a shift toward higher temperature and continued up to 250 °C at 20 °C/min. It could be attributed to the reduction of residence time. Additionally, the dehydration temperature was above 100 °C, may be due to the surface tension in biomass capillaries, which restricted the loss of water bound [25].

The similar pyrolysis processes at all heating rates were also observed from TG and DTG curves. As an example, the whole

Table 2
Main characteristics of spent lark mushroom substrate.

Ultimate analysis	Content (%)	Proximate analysis	Content (%)
Carbon	40.96	Moisture	10.7
Hydrogen	4.93	Volatiles	72.1
Nitrogen	1.15	Fix carbon	8.1
Oxygen[a]	52.96	Ash	9.1

[a] Calculated by difference.

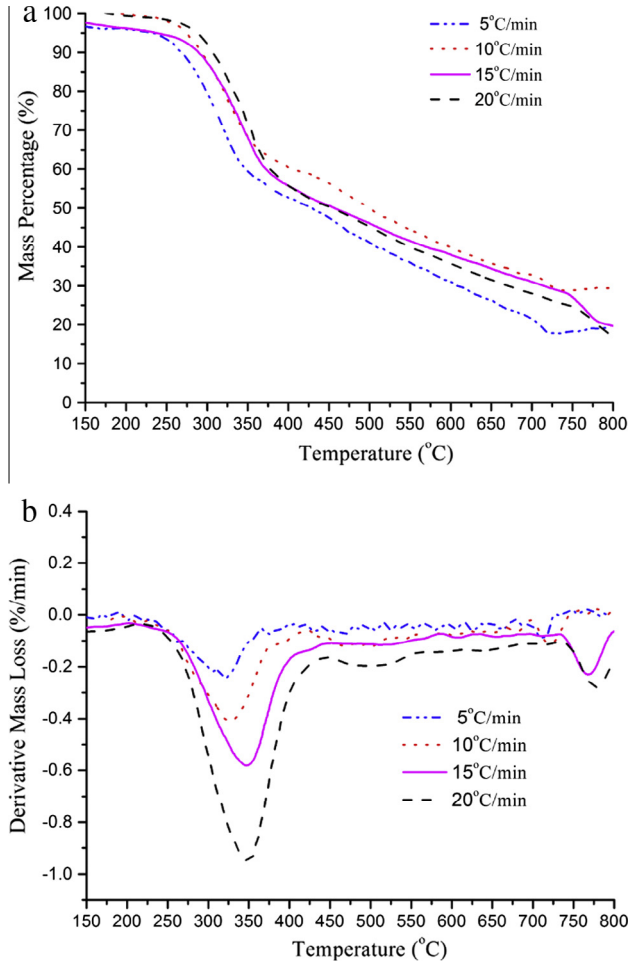

Fig. 2. TG and DTG plots of spent lark mushroom substrate at different heating rates, (a) TG; and (b) DTG.

thermal decomposition process at heating rate of 15 °C/min could be outlined as three stages without considering the release of moisture. Before 250 °C, the weight loss was mild. When temperature was above 265 °C, the mass loss began to accelerate and ended at around 380 °C. On the one hand, it could be attributed to the decomposition of cellulose and hemicellulose in raw material. This temperature zone was advantageous to facilitate the reaction of the depolymerization, for instance, the glycosidic bond in cellulosic was easier to be broken at this temperature range. At the same time, CO, CO_2 and other carbonaceous matters were formed [26]. On the other hand, the disintegration of a large number of carbon-containing constituents forced the mass loss rate to a maximum, which was found at 348 °C. Whereas, the degradation peaks of cellulose and hemicellulose in the sample were not separated obviously. It may be due to the partial overlap of thermal processes, which led to the presence of a shoulder peak not a well-defined peak [27]. At the range of 380–580 °C, there was a broad shoulder. It may be caused by breaking the bonds in some small polymers. Meanwhile, the hydrocarbons also began to form in this temperature zone. In the final stage (from 590 to 750 °C), an obvious weight loss was observed at higher temperature. According to the literature, it supposed that the weight loss was caused by the presence of secondary reactions, such as cracking, re-polymerization and re-condensation. These reactions would promote the charring processes of sample [28,29]. It should be noted that it was difficult to describe the thermal composition process distinctly, because of the complexity of biomass component. In the future work, more investigations would be carried out to elaborate the pyrolysis behavior in detail.

Table 3 displayed the characteristic parameters of major reaction stages. As the heating rate increased from 5 to 15 °C/min, the final pyrolysis temperature (T_f) at any thermal stage was shifted to the higher temperature. Moreover, the temperature which corresponded to the maximum weight loss rate (T_{max}), was also increased from 322 to 349 °C in the first stage and 467–512 °C in the second stage. The reason of the results could be explained by the effect of heat transfer. At lower heating rate, the whole biomass particle could develop a uniform temperature distribution due to the long residence time. With the raising of heating rate, temperature gradient existed between its surface and core, since the heat-conducting property of biomass was poor. Additionally, the insufficient residence time also urged the release of volatile matters at a higher temperature. Likewise, when the heating rate continued to rise, the average degradation rate (AR) also increased with 5.39 and 1.45%/min, respectively. These were probably attributed to the short residence time, which had been mentioned in the section above. The opinions were agreement with other researchers [28,30,31].

3.3. Kinetic analysis

Fig. 3 depicted the linear plots of $\ln\left[-\frac{\ln(1-x)}{T^2}\right]$ versus $\frac{1}{T}$. It showed good relatedness, and the correlation coefficients ranged from 92% to 99% which indicated the reliability of calculation in the first-order reaction model [18]. Table 4 listed the results of apparent activation energy and pre-exponential factor. It should be emphasized that there were two kinetic expressions for each heating rate, which represented the main thermal degradation stages of SLMS. From Table 4, it could be seen that in the first stage, the values of E_1 were between 54.42 and 77.26 kJ/mol. The mean value of apparent activation energy was 68.99 kJ/mol. Compared with other biomass and biomass wastes in literature, the obtained value was lower. For example, Gai et al. [32] investigated the thermal kinetics of corn straw and rice husk, the values of apparent activation energy were 79 and 129 kJ/mol, respectively. In the study of Van de Velden et al. [33], the kinetics of pyrolysis of two kinds of

Table 3
Pyrolysis parameters at different heating rates.

Heating rate (°C/min)	S_1				S_2			
	T_i (°C)	T_f (°C)	T_{max} (°C)	AR (%/min)	T_i (°C)	T_f (°C)	T_{max} (°C)	AR (%/min)
5	232	352	322	1.49	352	563	467	0.72
10	249	361	327	2.89	361	576	501	1.41
15	265	380	348	4.56	380	580	510	1.44
20	267	382	349	6.88	382	582	512	2.17

S_1: the first stage at any heating rate; S_2: the second stage at any heating rate; T_i: the initial temperature at any stage; T_f: the final temperature at any stage; T_{max}: the temperature corresponded to the maximum weight loss rate at any stage; AR: the average degradation rate at any stage.

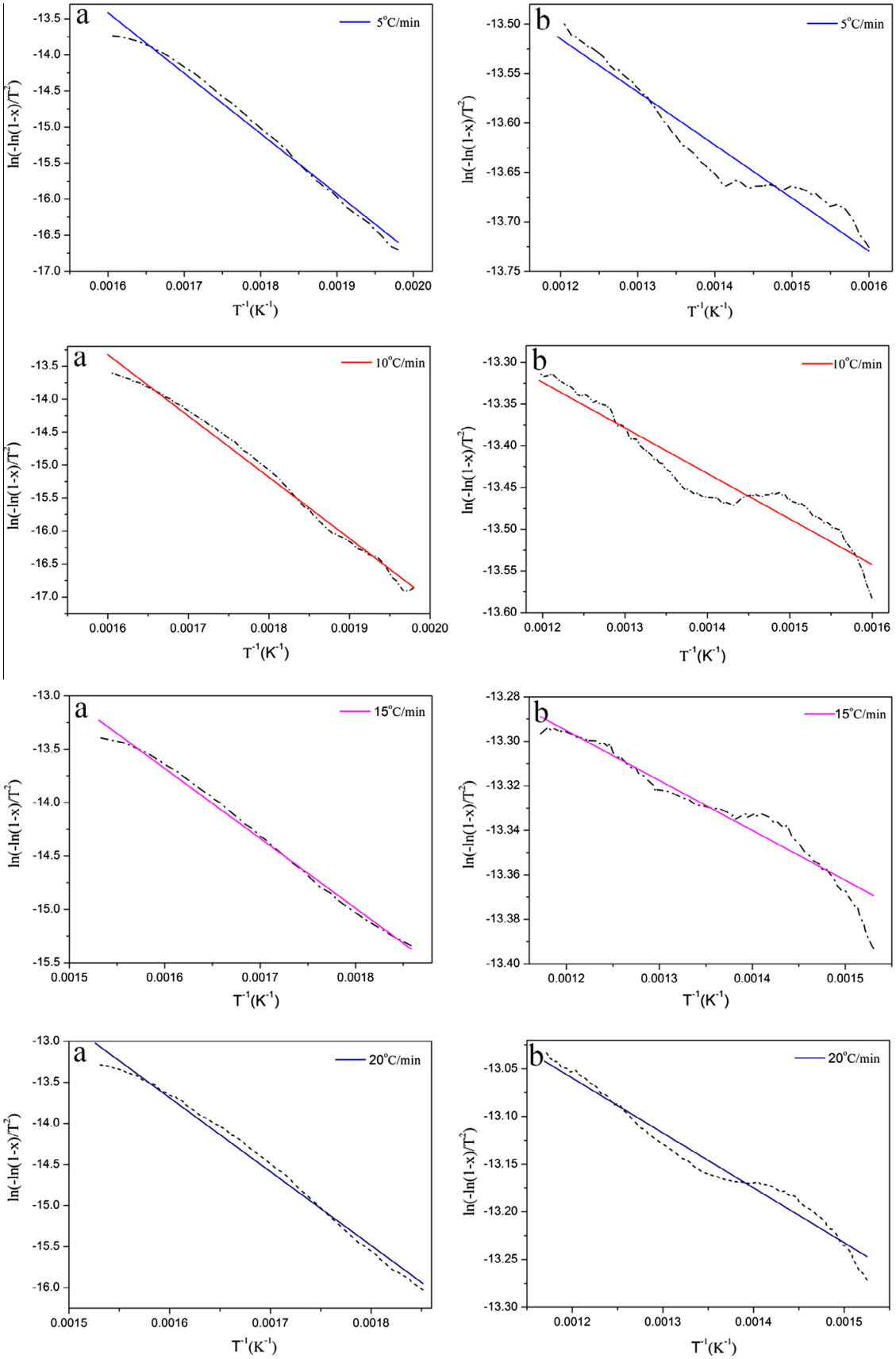

Fig. 3. Fitting curves at different pyrolysis temperature zones, (a) S_1; and (b) S_2.

biomass (sawdust and straw) was evaluated by using TGA and DSC instrument. The corresponding values of E_a were 75.8 and 76.3 kJ/mol. Amutio et al. [34] reported that the change range of E_a values of pinewood wastes was between 62 and 206 kJ/mol. Since the apparent activation energy, as a parameter, reflected the minimum energy required to break down the chemical bonds between atoms, the lower activation energy values in this study indicated it was easier to process the corresponding pyrolysis reaction.

In addition, from the table, it was also observed that the values of E_2 were around 4.6 kJ/mol (the values at 15 °C/min were not considered, because of large fluctuation). The value was consistent with the depiction of the pyrolysis process in the second stage (in Section 3.2). Furthermore, the maximum value of apparent activation energy was found at the highest heating rate. Although the maximum value of E_1 was not obtained at the same heating rate, the whole trend that the apparent activation energy were maintained at a high level at high heating rate (20 °C/min) was similar. This should be explained that due to the short residence time, high apparent activation energy was necessary to conquer the potential barrier of various chemical reactions, such as ring-opening, depolymerization and repolymerization [33]. In addition, according to the study of thermal behavior on Arundo donax, Jeguirim and Trouvé [35] had found that the delay only affected the thermal degradation process of cellulose and lignin. It had no influence on total mass loss. The similar results had also been reported in the investigations of other biomass resources. Therefore, the heating rate effect on liquid yield was not studied in the next work.

3.4. Production yields at different temperatures

The average yields of pyrolysis productions at 410, 430, 450, 470, 500 and 530 °C were shown in Fig. 4. The bio-oil yields varied between 8.6 and 14.4 wt.%. And, the yields of char and gas were 41.52–57.84 wt.% and 25.46–39.48 wt.%, respectively. From the data, the variation range of bio-oil yields was smaller than that of char and gas. This probably concerned with the thermal process of biomass. The major fraction of volatiles (approximately 40%) had been released from the sample before 382 °C, which indicated by the data of TG at heating rate of 20 °C/min. When temperature continued to rise, the more heat energy was obtained to promote the decomposition of solid char. Thus, some chars started to decompose and converted into gas. These caused the increase of bio-oil and gas yields. However, the temperature rose of up to 470 °C, the target liquid product yield was gradually decreased, which was attributed to the decomposition of the organic matter and the secondary thermal cracking process of bio-oil [13].

3.5. Ultimate analysis of bio-oil

Table 5 summarized the main element contents in bio-oil obtained at 470 °C. From Table 5, the oxygen and hydrogen content were 21.72% and 7.16%, respectively. The value of oxygen was lower than that of raw material. However, the hydrogen content was higher. Moreover, compared with the those produced by other biomass and biomass wastes [1,13,14], the variations of oxygen and hydrogen content in bio-oil were favorable, because they were beneficial to increase the higher heating value of liquid production. Besides, in comparison with conventional fuels, the H/C ratio indicated the obtained bio-oil lie between light and heavy petroleum products [36].

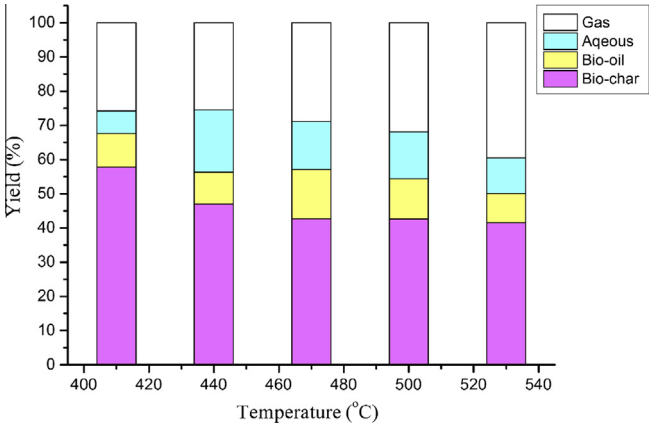

Fig. 4. Yields of pyrolysis productions at different final pyrolysis temperatures (feeding rate: 0.36 g/min, gas flow rate: 16 L/h).

Table 5
Main Characterization of bio-oil.

Ultimate analysis	Content (%)	Characterization	Content (%)
Carbon	65.29	HHV(MJ/kg)	24.82
Hydrogen	7.16	LHV(MJ/kg)	23.26
Nitrogen	5.83	H/C	1.32
Oxygen[a]	21.72	O/C	0.25

[a] By difference.

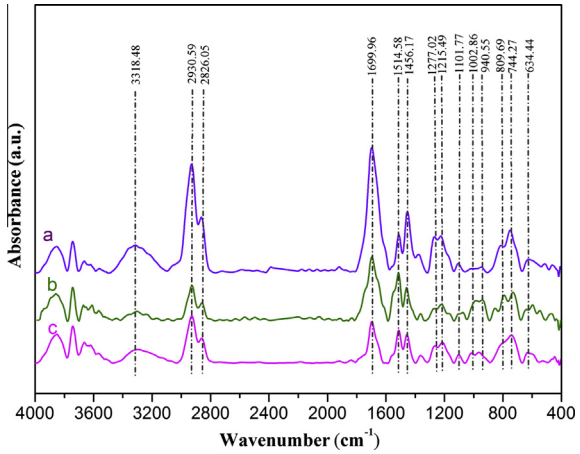

Fig. 5. FT-IR spectra of bio-oil at different final pyrolysis temperatures, (a) 440 °C; (b) 470 °C; and (c) 500 °C.

Table 4
Thermal kinetic parameters of raw material at different stages.

Heating rate (°C/min)	S_1			S_2		
	E_1 (kJ/mol)	A_1 (min^{-1})	R^2	E_2 (kJ/mol)	A_2 (min^{-1})	R^2
5	69.57	4.06×10^5	0.9885	4.46	6.9×10^{-3}	0.9323
10	77.26	4.35×10^6	0.9901	4.54	1.72×10^{-2}	0.9231
15	54.42	3.36×10^5	0.9939	1.86	7.41×10^{-3}	0.9491
20	74.74	3.61×10^6	0.9893	4.79	4.89×10^{-2}	0.9715

E_i: the apparent activation energy at any stage; A_i: the pre-exponential factor at any stage; R^2: the correlation coefficient.

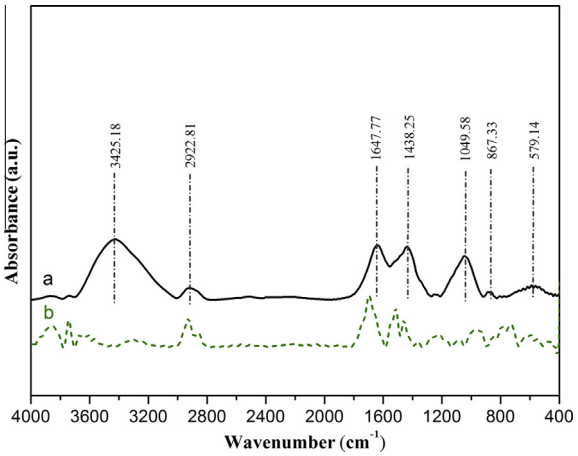

Fig. 6. The FT-IR spectra of raw material and bio-oil, (a) SMLS; and (b) bio-oil.

Table 6
The tentative components in bio-oil.

Chemical component	RT (min)	Peak area (%)
Spiropentane	5.213	0.23
Benzaldehyde	6.762	0.37
Phenol	7.464	3.86
Methylamine, N-(1-methylhexylidene)-	8.008	0.23
2-Cyclopenten-1-one,2-hydroxy-3-methyl-	8.416	0.38
2-Pentenenitrile, 5-hydroxy, (E)-	8.699	0.20
Phenol,2-methyl-	9.086	0.81
Phenol,3-methyl-	9.505	1.21
5-Ethyl-2-furaldehyde	9.715	1.60
N-[6-[N-aziridyl]-3-aza-3hexenyl]morpholine	10.437	0.36
5-Acetylpyrimidine	10.667	0.17
Phenol,3,5-dimethyl-	10.835	0.41
Phenol,2-ethyl-	11.149	2.92
Benzene,1,4-dimethoxy-	11.557	0.33
Ethanedithioamide	11.997	0.76
Phenol,3-(1-methylethyl)-	12.290	0.21
Phenol,4-ethyl-2-methoxy-	12.887	0.88
Indole	13.107	0.19
Phenol,2,3,5,6-tetramethyl-phenol	13.400	0.73
Cyclohexasiloxane, dodecamethyl-	13.588	0.38
Biphenyl	13.923	0.53
3-lsopropoxy-1,1,1,7,7,7-hexamethyl-3,5,5-tris(trimethylsiloxy)tetra	15.871	0.48
Trans-2-undecenoic acid	15.902	0.46
Thiophene,2-heptyl-	18.300	0.18
1,2-benzenedicarboxylic acid	21.346	0.65

3.6. The analysis of FT-IR spectra

Because of the similar tendency, our work just selected three typical FT-IR spectra showed in Fig. 5, which demonstrated that the influence of temperature on functional group types in bio-oil was slight. The broad absorbance peak (near 3318 cm^{-1}) was the O—H stretching vibration, which suggested the presence of carboxylic acids and alcohols. The peaks (between 2826 and 2930 cm^{-1}) were corresponded to C—H stretching vibration of aliphatic methylene groups. It may be caused by the thermal decomposition of cellulose in sample [37]. A strong absorbance peak (about 1700 cm^{-1}) was associated with the ketonic functional groups. Both C=C stretching vibration peaks between 1450 and 1600 cm^{-1} and C—H 'out of plane' peaks between 740 and 810 cm^{-1} indicated the presence of aromatic structures in bio-oil.

The spectrum of SLMS was shown in Fig. 6, compared to that of bio-oil, the spent lark mushroom substrate existed less types of functional groups. The peaks near 3425, 2923, 1648, 1049 and 867 cm^{-1} indicated the presence of phenolic, aliphatic, ketonic, alcohol and other aromatic compounds, respectively.

3.7. GC/MS analysis

In order to recognize the chemical components in the bio-oil, the technology of GC/MS was used. The tentative components of bio-oil obtained at 470 °C were listed in Table 6. As seen from Table 6, the peak areas of phenol and its derivatives dominated the results of the selected components. The reason was mainly due to the conversion of some lignin structures in raw material. In addition, the aromatic and oxygenated compounds were observed, including 1,2-benzenedicarboxylic acid, biphenyl, 1,4-dimethoxy benzene, etc. This could be explained by the degradation of oxygenated components. The presence of 5-ethyl-2-furaldehyde was considered to be the decomposition of cellulose. Other chemical compounds such as spiropentane, indole, 5-acetylpyrimidine, butylcitrate, ethanedithioamide, were also found. Therefore, after further upgrading, the most of the bio-oil components could be utilized as chemical feedstock or production [38].

4. Conclusions

In this study, the thermal behavior of spent lark mushroom substrate was analyzed by the TG and DTG curves at different heating rates. An iso-conversional model was adopted for evaluating the kinetics of thermal degradation of biomass. The results showed that the thermal decomposition process of SLMS was mainly concentrated on the first stage. Meanwhile, the average apparent activation energy in the first stage was 68.99 kJ/mol. The lower activation energy values indicated it was easier to process the corresponding pyrolysis reaction.

The optimum final pyrolysis temperature was determined at 470 °C with the bio-oil yield of 14.4 wt.%. The content of hydrogen maintained a specific advantage compared with other biomass pyrolysis oils. The ratio of H/C had shown that the obtained bio-oil lie between those of light and heavy petroleum products. According to the analysis of FT-IR and GC/MS, it demonstrated that the phenol and its derivatives occupied an important proportion. Otherwise, the chemical components such as 1,2-benzenedicarboxylic acid, biphenyl and indole were also observed. After upgrading, the chemical components in bio-oil could be utilized in many fields. In short, the bio-oil obtained from spent lark mushroom substrate could act as a kind of synthetic fuels or chemical feedstock to be used in the future.

Acknowledgements

The authors are grateful to Basic Research Program of Jilin Provincial Science and Technology Department (20130102040JC), Changchun Science and Technology Project (13NK01) and Resource Evaluation Sector of China Geological Survey for financial support (Grant 1212011220797). We also appreciate Yongqiang Zhang, Zaihang Zheng and Sunhua Deng for providing writing assistance for this study.

References

[1] Yin R, Liu R, Mei Y, Fei W, Sun X. Characterization of bio-oil and bio-char obtained from sweet sorghum bagasse fast pyrolysis with fractional condensers. Fuel 2013;112:96–104.
[2] Shi X-S, Yuan X-Z, Wang Y-P, Zeng S-J, Qiu Y-L, Guo R-B, et al. Modeling of the methane production and pH value during the anaerobic co-digestion of dairy manure and spent mushroom substrate. Chem Eng J 2014;244:258–63.
[3] Abnisa F, Arami-Niya A, Wan Daud WMA, Sahu JN, Noor IM. Utilization of oil palm tree residues to produce bio-oil and bio-char via pyrolysis. Energy Convers Manage 2013;76:1073–82.

[4] Horne PA, Williams PT. Influence of temperature on the products from the flash pyrolysis of biomass. Fuel 1996;75:1051–9.
[5] Antonakou E, Lappas A, Nilsen MH, Bouzga A, Stöcker M. Evaluation of various types of Al-MCM-41 materials as catalysts in biomass pyrolysis for the production of bio-fuels and chemicals. Fuel 2006;85:2202–12.
[6] Ren X, Meng J, Moore AM, Chang J, Gou J, Park S. Thermogravimetric investigation on the degradation properties and combustion performance of bio-oils. Bioresour Technol 2014;152:267–74.
[7] Pattiya A, Suttibak S. Influence of a glass wool hot vapour filter on yields and properties of bio-oil derived from rapid pyrolysis of paddy residues. Bioresour Technol 2012;116:107–13.
[8] Mohan D, Sharma R, Singh VK, Steele P, Pittman CU. Fluoride removal from water using bio-char, a green waste, low-cost adsorbent: equilibrium uptake and sorption dynamics modeling. Ind Eng Chem Res 2012;51:900–14.
[9] Lappas VSDAA, Antonakou EV, Voutetakis SS, Vasalos IA. Design, construction, and operation of a transported fluid bed process. Process Des Control 2008;47:742–7.
[10] Sait HH, Hussain A, Salema AA, Ani FN. Pyrolysis and combustion kinetics of date palm biomass using thermogravimetric analysis. Bioresour Technol 2012;118:382–9.
[11] Huang YF, Chiueh PT, Kuan WH, Lo SL. Pyrolysis kinetics of biomass from product information. Appl Energy 2013;110:1–8.
[12] Ceylan S, Topçu Y. Pyrolysis kinetics of hazelnut husk using thermogravimetric analysis. Bioresour Technol 2014;156:182–8.
[13] Salehi JAE, Harding T. Bio-oil from sawdust-pyrolysis of sawdust in a fixed-bed system. Energy Fuels 2009:3767–72.
[14] Yanik J, Kornmayer C, Saglam M, Yüksel M. Fast pyrolysis of agricultural wastes: characterization of pyrolysis products. Fuel Process Technol 2007;88:942–7.
[15] Manuel Garcia-Perez XSW, Shen Jun, Rhodes Martin J, Fujun Tian W-JL, Wu Hongwei, Li Chun-Zhu. Fast pyrolysis of oil mallee woody biomass-effect of temperature on the yield. Chem Res 2008;47.
[16] Dewayanto N, Isha R, Nordin MR. Use of palm oil decanter cake as a new substrate for the production of bio-oil by vacuum pyrolysis. Energy Convers Manage 2014;86:226–32.
[17] Uzun BB, Sarioğlu N. Rapid and catalytic pyrolysis of corn stalks. Fuel Process Technol 2009;90:705–16.
[18] Çepelioğullar Ö, Pütün AE. Thermal and kinetic behaviors of biomass and plastic wastes in co-pyrolysis. Energy Convers Manage 2013;75:263–70.
[19] Vamvuka D, Troulinos S, Kastanaki E. The effect of mineral matter on the physical and chemical activation of low rank coal and biomass materials. Fuel 2006;85:1763–71.
[20] Lapuerta Mn, Hernández JJ, Rodríguez Jn. Kinetics of devolatilisation of forestry wastes from thermogravimetric analysis. Biomass Bioenergy 2004;27:385–91.
[21] Asadullah M, Ab Rasid NS, Kadir SASA, Azdarpour A. Production and detailed characterization of bio-oil from fast pyrolysis of palm kernel shell. Biomass Bioenergy 2013;59:316–24.
[22] Sheng C, Azevedo JLT. Estimating the higher heating value of biomass fuels from basic analysis data. Biomass Bioenergy 2005;28:499–507.
[23] Zema DA, Bombino G, Andiloro S, Zimbone SM. Irrigation of energy crops with urban wastewater: effects on biomass yields, soils and heating values. Agric Water Manage 2012;115:55–65.
[24] Alvarez J, Lopez G, Amutio M, Bilbao J, Olazar M. Bio-oil production from rice husk fast pyrolysis in a conical spouted bed reactor. Fuel 2014;128:162–9.
[25] Safi MJ, Mishra IM, Prasad B. Global degradation kinetics of pine needles in air. Thermochim Acta 2004;412:155–62.
[26] Banyasz JL, Li S, Lyons-Hart JL, Shafer KH. Cellulose pyrolysis: the kinetics of hydroxyacetaldehyde evolution. J Anal Appl Pyrolysis 2001;57:223–48.
[27] Popescu C-M, Spiridon I, Tibirna CM, Vasile C. A thermogravimetric study of structural changes of lime wood (Tilia cordata Mill.) induced by exposure to simulated accelerated UV/Vis-light. J Photochem Photobiol A: Chem 2011;217:207–12.
[28] Maiti S, Purakayastha S, Ghosh B. Thermal characterization of mustard straw and stalk in nitrogen at different heating rates. Fuel 2007;86:1513–8.
[29] Părpăriţă E, Brebu M, Azhar Uddin M, Yanik J, Vasile C. Pyrolysis behaviors of various biomasses. Polym Degradat Stability 2014;100:1–9.
[30] Şensöz S, Angın D. Pyrolysis of safflower (Charthamus tinctorius L.) seed press cake in a fixed-bed reactor: Part 2. Structural characterization of pyrolysis bio-oils. Bioresour Technol 2008;99:5498–504.
[31] Manyà JJ, Roca FX, Perales JF. TGA study examining the effect of pressure and peak temperature on biochar yield during pyrolysis of two-phase olive mill waste. J Anal Appl Pyrolysis 2013;103:86–95.
[32] Gai C, Dong Y, Zhang T. The kinetic analysis of the pyrolysis of agricultural residue under non-isothermal conditions. Bioresour Technol 2013;127:298–305.
[33] Van de Velden M, Baeyens J, Brems A, Janssens B, Dewil R. Fundamentals, kinetics and endothermicity of the biomass pyrolysis reaction. Renewable Energy 2010;35:232–42.
[34] Amutio M, Lopez G, Aguado R, Artetxe M, Bilbao J, Olazar M. Kinetic study of lignocellulosic biomass oxidative pyrolysis. Fuel 2012;95:305–11.
[35] Jeguirim M, Trouvé G. Pyrolysis characteristics and kinetics of Arundo donax using thermogravimetric analysis. Bioresour Technol 2009;100:4026–31.
[36] Şensöz S, Angın D, Yorgun S. Influence of particle size on the pyrolysis of rapeseed (Brassica napus L.): fuel properties of bio-oil. Biomass Bioenergy 2000;19:271–9.
[37] Naik S, Goud VV, Rout PK, Jacobson K, Dalai AK. Characterization of Canadian biomass for alternative renewable biofuel. Renewable Energy 2010;35:1624–31.
[38] Dinesh Mohan Jr CUP, Steele Philip H. Pyrolysis of wood biomass for bio-oil- a critical review. Energy Fuels 2006:848–89.